

High Energy Large Area Surveys: from BeppoSAX to Chandra and XMM-Newton

Fabrizio Fiore^{a*}

^aINAF - Osservatorio Astronomico di Roma
via Frascati 33, Monteporzio (Rm) I00040 Italy

Hard X-ray observations are the most efficient way to discriminate accretion-powered sources from star-light. Furthermore, hard X-rays are less affected than other bands by obscuration. For these reasons the advent of imaging instruments above 2 keV, has permitted to dramatically improve our understanding of accretion-powered sources and their cosmic evolution. By minimizing the problems of AGN selection and nuclear obscuration, the combination of deep and shallow hard X-ray surveys, performed first with ASCA and BeppoSAX and then with Chandra and XMM (e.g. ASCA LSS, HELLAS, CDFN, CDFS, Lockman Hole, SSA13, HELLAS2XMM etc.), allows a detailed study of the evolution of accreting sources. Somewhat surprising results are emerging: 1) the sources making the Cosmic X-ray Background peak at a redshift ($z=0.7-1$) lower than soft X-ray selected sources and lower than predicted by synthesis models for the CXB; 2) there is strong evidence of a luminosity dependence of the evolution, low luminosity sources (i.e. Seyfert galaxies) peaking at a significantly later cosmic time than high luminosity sources.

1. INTRODUCTION

Hard X-ray surveys are the most direct probe of supermassive black hole (SMBH) accretion activity, which is recorded in the Cosmic X-ray Background (CXB), in wide ranges of SMBH masses, down to $\sim 10^6 - 10^7 M_\odot$, and bolometric luminosities, down to $L \sim 10^{43}$ erg/s. At $z \gtrsim 0.5$, these regimes of accretion are hardly accessible to optical observations but may provide a significant fraction of the total accretion power of the Universe. X-ray surveys can therefore be used to constrain the SMBH mass density, models for the CXB [1,2,3], and models for the formation and evolution of the structure in the universe [4,5].

The advent of imaging instruments in the 2-10 keV band, first aboard ASCA and BeppoSAX and then on Chandra and XMM-Newton, has led to a dramatic advance. ASCA and BeppoSAX shallow surveys have resolved about 20 % of the 2-10 keV and 5-10 keV CXB, while Chandra and XMM-Newton deep surveys have resolved 80-90%

of the 2-10 keV CXB [6,7,8,9,10,11,12,13,14,15, 16,17]. A detailed study of the cosmic evolution of the hard X-ray source population is being pursued combining source identifications from both shallow and deep surveys. These studies confirm, at least qualitatively, the predictions of standard AGN synthesis models for the CXB: the 2-10 keV CXB is mostly made by the superposition of obscured and unobscured AGN [9,18,11,19,20, 16,21]. Quantitatively, though, rather surprising results are emerging: a rather narrow peak in the range $z=0.7-1$ is present in the redshift distributions from ultra-deep Chandra and XMM-Newton pencil-beam surveys, in contrast to the broader maximum observed in previous shallower soft X-ray surveys (e.g. ROSAT, [22,23]) and predicted by the above mentioned synthesis models; furthermore, evidence is emerging (related to the difference above) of a luminosity dependence in the number density evolution of both soft and hard X-ray selected AGN.

The ultra-deep Chandra and XMM-Newton surveys of the Chandra Deep Field North (CDFN [15]), Chandra Deep Field South (CDFS [14]) and Lockman Hole (LH [16]) cover each $\sim 0.05 - 0.1$

*This work has been supported by ASI contracts I/R/107/00, I/R/037/01, and by Cofin-99-034, and CNAA 2000, 2001 grants

deg^2 . For this reason the number of high luminosity sources in these surveys is small, being the slope of the AGN luminosity function at high luminosities rather steep. As an example, in the CDFN there are only 6 AGN with $\log(L_{2-10\text{keV}}/\text{ergs}^{-1}) \gtrsim 44$ at $z > 3$ and 20 at $z > 2$ [24]. To compute an accurate luminosity function on wide luminosity and redshift intervals, and to find sizeable samples of “rare” objects, such as high luminosity, highly obscured type 2 QSO or X-ray bright, optically normal galaxies, XBONGs [25,26], a much wider area needs to be covered, of the order of a few deg^2 . To this purpose several high energy, large area, medium-deep surveys are being pursued, like, for example, the: HELLAS2XMM serendipitous survey, which, using XMM-Newton archival observations [27] has the goal to cover $\sim 4 \text{ deg}^2$ at a 2-10 keV flux limit of a few $\times 10^{-14} \text{ erg cm}^{-2} \text{ s}^{-1}$; the XMM Bright Sample Survey, with the goal of covering $\sim 50 \text{ deg}^2$ at the flux limit of a few $\times 10^{-13} \text{ erg cm}^{-2} \text{ s}^{-1}$, using again XMM-Newton archive observations; the ELAIS-S1 XMM survey, which covers a contiguous area of 0.5 deg^2 at a flux limit of a few $\times 10^{-15} \text{ erg cm}^{-2} \text{ s}^{-1}$; the COSMOS-VIMOS-XMM survey, which will cover a contiguous area of $\sim 2 \text{ deg}^2$ at a similar flux limit. Other relevant Chandra project include: the Chandra serendipitous survey “Champ”, which covers $\sim 14 \text{ deg}^2$ at a 2-10 keV flux limit of a few $\times 10^{-14} \text{ erg cm}^{-2} \text{ s}^{-1}$ ([28]); the Chandra serendipitous survey SEXSI ([29]); the Chandra-SWIRE survey of the Lockman field; the extended Chandra survey of the CDFS region.

2. THE BEPPoSAX HERITAGE

BeppoSAX pioneered the study of the hard X-ray sky using both its imaging telescopes (the 5-10 keV HELLAS survey) and its collimated instruments (the 13-200 keV PDS survey of nearby AGN and blank fields). We briefly review these two topics in the following.

2.1. The hard X-ray sky faint source population

The BeppoSAX HELLAS survey covers $\sim 85 \text{ deg}^2$ of the sky down to a 5-10 keV flux of

$5 \times 10^{-14} \text{ erg cm}^{-2} \text{ s}^{-1}$ [10]. Fig. 1 compares the integral 5-10 keV logN-logS of the 147 HELLAS sources with that obtained from deeper XMM surveys. We have obtained the optical identification of about half (62) of the sources in a reduced area of sky (55 deg^2) with $\delta < +79^\circ$, $20\text{hr} < \alpha < 5\text{hr}$ and $6.5\text{hr} < \alpha < 17\text{hr}$ [11]. Because of the quite large MECS error box ($\sim 1'$ radius), we limited the optical identification process to objects with surface density $\lesssim 40 \text{ deg}^{-2}$, to keep the number of spurious identifications in the whole sample smaller than a few percent. While broad line AGN are identified up to $z=2.76$, all narrow line AGN have $z < 0.4$, due to the conservative threshold adopted for the optical magnitude of narrow emission line AGN and galaxies (which do not show a bright optical nucleus, because of the strong extinction). The fraction of highly obscured sources ($N_H \gtrsim 10^{23}$) at $z < 0.3$ (where our survey should be representative of the actual source population), is $\sim 40\%$, consistent with the expectations of AGN synthesis models [3]. In this redshift range all highly obscured objects are narrow line AGN and galaxies, while all broad line AGN have $N_H < 10^{23} \text{ cm}^{-2}$, consistent with popular AGN unification schemes. The situation is somewhat different at high redshift, where we found indications of low energy absorption in a few broad line AGNs [10]. Obscured, broad line AGNs at high z have been discovered by ROSAT [30,31] ASCA [8] and are found in deeper XMM and Chandra surveys [32,33]. Possible explanations for the optical/X-ray dichotomy can be found in [34].

2.2. The BeppoSAX PDS view of highly obscured AGNs

The faint sources discovered by the BeppoSAX MECS are not accessible to the BeppoSAX PDS [35], which is limited to 13-80 keV fluxes higher than $\sim 10^{-11} \text{ erg cm}^{-2} \text{ s}^{-1}$. However, this is some 30 times deeper than the HEAO1-A4 survey, and deeper than any previous (and current!) satellite based experiment in this energy range. For this reason the PDS observations of extragalactic sources have opened up a new space of discovery and are a reference point for high energy AGN studies. The BeppoSAX PDS has

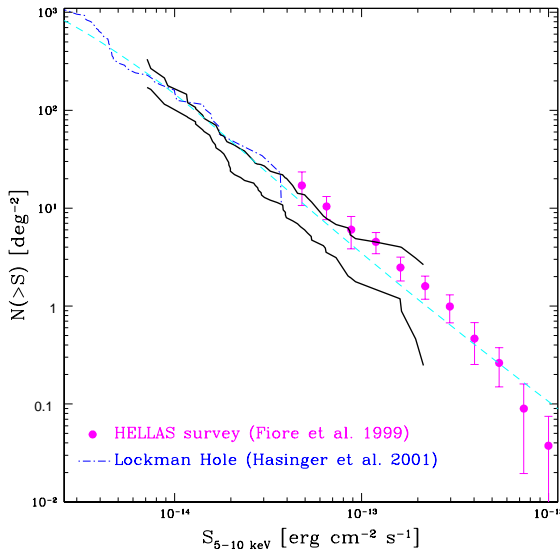


Figure 1. The 5-10 keV number counts from the BeppoSAX HELLAS survey, filled points [10], the HELLAS2XMM survey, region inside the solid lines [27], and the XMM Lockman hole pointing, dot-dashed line [16].

detected some 100 AGN above 13 keV, a factor of 5-10 improvement with respect to previous observations. About 35 of these objects show strong obscuration at lower energies [36,37], see also Matt, these proceedings. Fig. 2 show two examples, the archetypal Seyfert 2 galaxy NGC1068 and the ultra-luminous infrared galaxy NGC6240. The presence of a highly obscured, and intrinsically very luminous active nucleus in the latter source was assessed thanks to this BeppoSAX PDS observation [38] (the optical spectrum of NGC6240 is typical of a LINER). Similar observations were performed by several other authors, see e.g. [36,39,40].

The PDS has also performed a survey of about 200 deg² of the high Galactic latitude sky down to its flux limit, using the off-source pointings (the PDS consists of four phoswich units and is operated in the so called “rocking mode”, with a pair of units pointing to the source while the other

pair monitors the background ± 210 arcmin away; the units on and off are interchanged every 96 seconds). A fluctuation analysis of the PDS off-source pointings estimates in 0.02-0.06 the number of sources per deg² with 13-80 keV flux higher than 10^{-11} erg cm⁻² s⁻¹. This is in agreement with the extrapolation of the HELLAS 5-10 keV logN-logS in the 13-80 keV band if a power law spectrum with $\alpha_E = 0.8$ and reduced at low energy by a column density of $1 - 3 \times 10^{23}$ cm⁻², consistent with the expectation of AGN synthesis models for the CXB [3], is assumed.

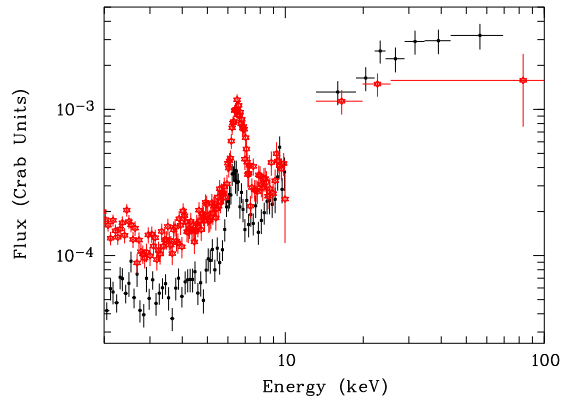


Figure 2. Comparison of the BeppoSAX MECS and PDS spectra of NGC1068 (open stars) with those of NGC6240 (dots). Both spectra have been normalized to the Crab spectrum. Adapted from Vignati et al. 1999 [38]

3. THE HELLAS2XMM SURVEY

The natural extension of the BeppoSAX HELLAS survey to ~ 10 lower X-ray fluxes, where the bulk of the CXB is resolved in sources, made use of the higher throughput and much better source localization (a few arcsec) of the XMM-Newton telescopes, which allowed the identification of X-ray sources with faint optical counterparts. We have obtained optical photomet-

ric and spectroscopic follow-up of 122 sources in five XMM-Newton fields, covering a total of 0.9 deg^2 (the HELLAS2XMM ‘1dF’ sample), down to a flux limit of $F_{2-10\text{keV}} \sim 10^{-14} \text{ erg cm}^{-2} \text{ s}^{-1}$. We found optical counterparts brighter than $R \sim 25$ within $\sim 6''$ from the X-ray position in 116 cases and obtained optical spectroscopic redshifts and classification for 94 of these sources [18]. The source breakdown includes: 61 broad line QSO and Seyfert 1 galaxies; 14 narrow line AGN (9 of which have $\log(L_{2-10\text{keV}}/\text{ergs}^{-1}) > 44$ and can therefore be considered type 2 QSO); 14 emission line galaxies, all with $\log(L_{2-10\text{keV}}/\text{ergs}^{-1}) > 42.7$ and therefore all probably hosting an AGN; 5 early type galaxies with $41.9 < \log(L_{2-10\text{keV}}/\text{ergs}^{-1}) < 43.0$, therefore XBONGs, all probably hosting an AGN; 1 star; 2 groups or clusters of galaxies. In the following we limit ourselves to consider two broad categories: *optically unobscured AGN*, i.e. type 1, broad emission line AGN, and *optically obscured AGN*, i.e. AGN whose nuclear optical emission, is totally or strongly reduced by dust and gas in the nuclear region and/or in the host galaxy.

We have combined the HELLAS2XMM 1dF sample with other deeper hard X-ray samples including: 1- CDFN sample from [20]: 120 sources with flux $F_{2-10\text{keV}} > 10^{-15} \text{ erg cm}^{-2} \text{ s}^{-1}$, 67 with a spectroscopic redshift. 2- Lockman Hole sample from [41,27]: 55 sources with $F_{2-10\text{keV}} > 4 \times 10^{-15} \text{ erg cm}^{-2} \text{ s}^{-1}$, 41 with a spectroscopic redshifts and 3 with a photometric redshifts; 3- SSA13 sample from [13,19]: 20 sources with $F_{2-10\text{keV}} > 3.8 \times 10^{-15} \text{ erg cm}^{-2} \text{ s}^{-1}$, 13 with spectroscopic redshift. Overall, we dealt with 317 faint hard X-ray selected sources, 221 (70%) of them identified with an optical counterpart whose redshift is available. This “combined” sample includes 113 broad line AGN and 108 optically obscured AGN.

Fig. 3 shows the X-ray (2-10 keV) to optical (R band) flux ratio (X/O) for the combined sample. About 20% of the sources have $X/O \gtrsim 10$, i.e. ten times or more higher than the X/O typical of optically selected AGN. At the flux limit of the HELLAS2XMM 1dF sample several sources with $X/O \gtrsim 10$ have optical magnitudes $R=24-25$,

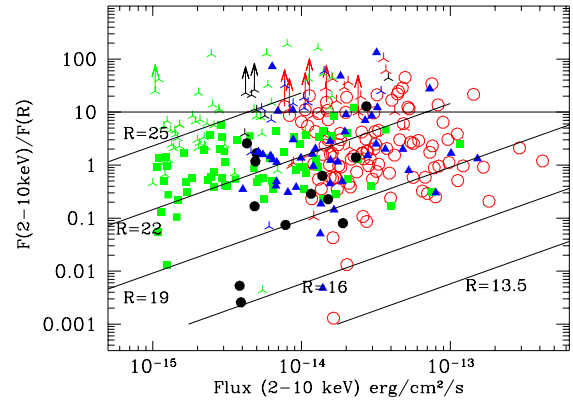


Figure 3. The X-ray (2-10 keV) to optical (R band) flux ratio X/O as a function of the X-ray flux for the combined sample (HELLAS2XMM = open circles; CDFN = filled squares; LH = filled triangles; SSA13 = filled circles, skeleton triangles are sources without a measured redshift). Solid lines mark loci of constant R band magnitude. The part of the diagram below the $R=25$ line is accessible to optical spectroscopy with 10m class telescopes. Note that $\sim 20\%$ of the sources have $X/O \gtrsim 10$, irrespective of the X-ray flux. HELLAS2XMM 1dF sources with $X/O \gtrsim 10$ have $R=24-25$, and therefore their redshifts can be measured through optical spectroscopy.

bright enough for reliable spectroscopic redshifts to be obtained with 8m class telescopes. Indeed, we were able to obtain spectroscopic redshifts and classification of 13 out of the 28 HELLAS2XMM 1dF sources with $X/O > 10$: 8 of them are type 2 QSO at $z=0.7-1.8$, to be compared with the total of 10 type 2 QSOs identified in the CDFN [24] and CDFS [21].

Fig. 4 show the X-ray to optical flux ratio as a function of the X-ray luminosity for broad line AGN (left panel) and non broad line AGN and galaxies (right panel). While the X/O of the broad line AGNs is not correlated with the luminosity, a striking correlation between $\log(X/O)$ and $\log(L_{2-10\text{keV}})$ is present for the obscured

AGN: higher X-ray luminosity, optically obscured AGN tend to have higher X/O. The solid diagonal line in the panel represents the best linear regression between $\log(\text{X/O})$ and $\log(L_{2-10\text{keV}})$. The nuclear optical-UV light is completely blocked, or strongly reduced in these objects, unlike the X-ray light. Indeed, the optical R band light of these objects is dominated by the host galaxy and therefore, *X/O is roughly a ratio between the nuclear X-ray flux and the host galaxy starlight flux*.

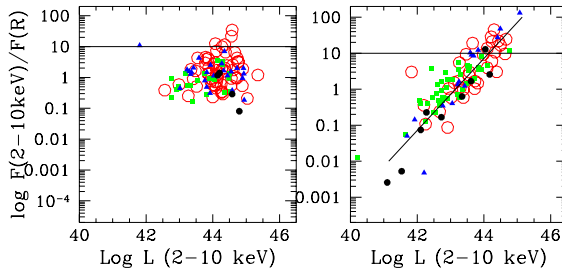


Figure 4. The X-ray to optical flux ratio versus the X-ray luminosity for type 1 AGN, left panel, and non type 1 AGN and galaxies, right panel. Symbols as in Fig. 3. The horizontal lines mark the level of $\text{X/O}=10$, $\sim 20\%$ of the sources in the combined sample have X/O higher than this value. The diagonal line in the right panel is the best $\log(\text{X/O})-\log(L_{2-10\text{keV}})$ linear regression.

4. THE EVOLUTION OF HARD X-RAY SELECTED AGNS

We can use the fractions of obscured to unobscured objects in the combined sample and the correlations in Fig. 4 to attribute, in a purely statistical sense, a luminosity, and therefore a redshift, to the sources in the combined sample without optical spectroscopic identification. The full combined sample (including both the objects with measured redshift and the objects with the statistically estimated redshift), complemented at high fluxes by 66 sources from the

HEAO1 A2 all sky survey [42] with $F_{2-10\text{keV}} > 2 \times 10^{-11} \text{ erg cm}^{-2} \text{ s}^{-1}$, has been used to compute the evolution of the number density of hard X-ray selected sources, using the standard $1/V_{\text{max}}$ method [43].

Fig. 5 plots the evolution of the number density in three luminosity bins: $\log(L_{2-10\text{keV}}/\text{ergs}^{-1}) = 43 - 44$, $\log(L_{2-10\text{keV}}/\text{ergs}^{-1}) = 44 - 44.5$ and $\log(L_{2-10\text{keV}}/\text{ergs}^{-1}) = 44.5 - 46$. The dashed lines are lower limits computed using only the sources with measured redshift. We see that the number density of lower luminosity AGN increases between $z=0$ and $z=0.5$ by a factor ~ 13 and stays approximately constant up to $z \sim 2$. Conversely, the number density of luminous AGN increases by a factor ~ 100 up to $z=2$ and by a factor ~ 170 up to $z \sim 3$. The last behaviour is similar to that of luminous ($M_B < -24$) optically selected QSO [44].

5. CONCLUSIONS

Thanks to both deep, pencil beam, and shallow but larger area high energy X-ray surveys performed in the past few years by BeppoSAX, ASCA, Chandra and XMM-Newton we now have little doubts that the CXB is due to the integrated contribution by (mainly) AGN and therefore that it may be regarded as the electromagnetic outcome of mass accretion onto SMBH in these galactic nuclei, along the cosmic history. We have been able to study the evolution of accreting sources of low (i.e. Seyferts) and high luminosity (i.e. QSOs) up to $z \approx 3$, to find that there is strong evidence of a luminosity dependence of the evolution, low luminosity sources (i.e. Seyfert galaxies) peaking at a significantly later cosmic time than high luminosity sources (also see [21] and Hasinger, these proceedings). To push this study to higher redshift and to derive separately the evolution of unobscured and obscured objects we need to perform wide and deep surveys. For example, in the HELLAS2XMM 1dF sample there are some thirty "optically obscured" AGN: 100-150 sources of this type would be sufficient to adequately figure their luminosity function over 2-3 luminosity dex and a few redshift bins. This is the goal of the extension of the optical follow-up

of the HELLAS2XMM survey from 1 to 4 deg², which should allow us to contrast the luminosity function of obscured and unobscured AGN, and to study their differential evolution up to $z \sim 2$. On the other hand, the ultra-deep but small area CDFN survey has provided so far only 6 AGN more luminous than $\log(L_{2-10\text{keV}}/\text{ergs}^{-1}) = 44$ at $z > 3$ and 20 at $z > 2$ [24]. Note that all of them have flux $\gtrsim 10^{-15}$ erg cm⁻² s⁻¹, suggesting that the most effective strategy to find high luminosity, high z AGN consists in increasing the area covered at $F_{2-10\text{keV}} = 1 - 5 \times 10^{-15}$ erg cm⁻² s⁻¹, rather than pushing the depth of the survey. Observing of the order of 1 deg² of sky at the above flux limit, would roughly increase by a factor of 10 the number of high z objects, a program which will be carried out by the ELAIS-S1 and COSMOS-VIMOS-XMM surveys.

The hard X-ray selected source's luminosity functions can be used to determine the SMBH mass density. Using a simple approach [24] we find a SMBH density of $4 - 5 \times 10^5 M_{\odot}$ Mpc⁻³, about 2-3 times higher than that estimated using optical surveys and by [24], but consistent with both that measured from the intensity of the CXB ([45] and references therein) and from local galaxies [46,47]. This implies that most of this accretion of mass takes place during ‘active’ phases, when the accreting matter radiates powerfully, giving rise to an AGN. However, below 10 keV we cannot see directly much ($\sim 50\%$) of this accretion luminosity, because it appears to be hidden behind layers of gas and dust. Indeed, the energy range where most of the CXB energy density resides (the 20-60 keV range) remains as of today essentially unprobed, and therefore the fraction of highly obscured objects is today poorly constrained. The result is that all estimates on the accretion luminosity in the Universe and of the SMBH mass density are based on extrapolation of measurements performed below 10 keV into the 20-60 keV band, making rough assumptions about the fraction of obscured AGNs. This situation stems from the lack, so far, of focusing instruments in this band. A mission capable of exploring the hard X-ray sky with focusing/imaging instrumentation would be able to reach 13-80 keV fluxes 100-200 times lower than

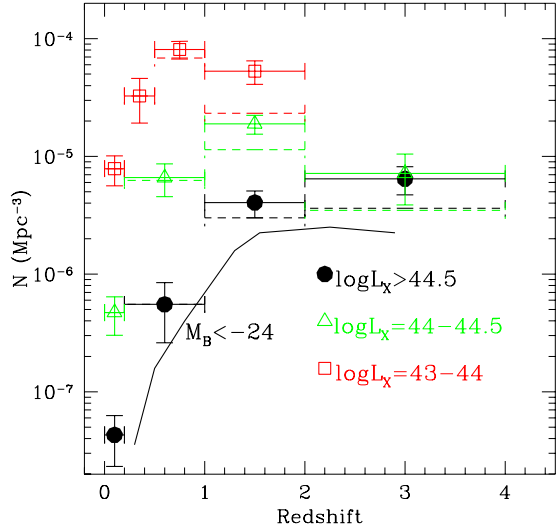


Figure 5. The evolution of the number density of hard X-ray selected sources in three bins of luminosity: $\log(L_{2-10\text{keV}}/\text{ergs}^{-1}) = 43 - 44 =$ empty squares; $\log(L_{2-10\text{keV}}/\text{ergs}^{-1}) = 44 - 44.5 =$ empty triangles; $\log(L_{2-10\text{keV}}/\text{ergs}^{-1}) > 44.5 =$ filled circles. Dashed lines represent lower limits obtained using only the sources with measured redshift, see the text. The solid continuous curve represents the evolution of optically selected QSO more luminous than $M_B = -24$ [44]. Note that the shape of the solid curve is similar to the evolution of the luminous X-ray selected sources.

those probed by the PDS, where the source density is ≈ 100 sources deg⁻², corresponding to resolving in sources roughly half of the CXB in that energy band. This would therefore lead to the solution of the longest standing issue in X-ray astronomy (and one of the most outstanding issue in Cosmology), by making a great leap forward, comparable to that achieved in the soft X-rays by the Einstein Observatory in the late 70'.

Acknowledgements. The original matter presented in this paper is the result of the effort of a large number of people, in particular of the HEL-

LAS and HELLAS2XMM teams. I would like to thank the BeppoSAX SOC, OCC and SDC teams for the successful operation of the BeppoSAX satellite, preliminary data reduction and screening, data calibration and archiving.

REFERENCES

1. Setti, G., & Woltjer, L. 1989, A&A, 224, L21
2. Comastri, A., Setti, G., Zamorani, G., & Hasinger, G. 1995, A&A, 296, 1
3. Comastri, A., Fiore, F., Vignali, C., Matt, G., Perola, G. C., & La Franca, F., 2001, MNRAS, 327, 781
4. Haehnelt, M. Carnegie Observatories Astrophysics Series, Vol. 1: Coevolution of Black Holes and Galaxies, ed. L. C. Ho (Cambridge Univ. Press), 2003, astro-ph/0307378
5. Menci, N., Cavaliere, A., Fontana, A., Giallongo, E., Poli, F., & Vittorini, V. 2003, ApJ, 587, L63
6. Ueda, Y., Takahashi, T., Ishisaki, Y., & Ohashi, T. 1999, ApJ, 524L, 11
7. Akiyama, M., et al. 2000, ApJ, 532, 700
8. Della Ceca, R., Castelli, G., Braito, V., Cagnoni, I., & Maccacaro, T. 1999, ApJ, 524, 674
9. Fiore, F., La Franca, F., Giommi, P., Elvis, M., Matt, G., Comastri, A., Molendi, S., & Gioia, I. 1999, MNRAS, 306, L55
10. Fiore, F., et al. 2001, MNRAS, 327, 771
11. La Franca, F., Fiore, F., Vignali, C., Antonelli, A., Comastri, A., Giommi, P., Matt, G., Molendi, S., Perola, G. C., & Pompilio, F. 2002, ApJ, 570, 100
12. Giommi, P., Perri, M., Fiore, F. 2000, A&A, 362, 799
13. Mushotzky, R.F., Cowie, L.L., Barger, A.J., & Arnaud, K.A. 2000, Nature, 404, 459
14. Giacconi, R., et al. 2002, ApJS, 139, 369
15. Brandt, W.N., et al. 2001 AJ, 122, 2810
16. Hasinger, G. et al. 2001, A&A, 365, L45
17. Alexander, D. et al. 2003, AJ, 126, 539
18. Fiore, F. Brusa, M, Cocchia, F. et al. 2003, A&A in press, astro-ph/0306556
19. Barger, A., Cowie, L., Mushotzky, R.F., & Richards, E.A. 2001, AJ, 121, 662
20. Barger A., et al. 2002, AJ, 124, 1839
21. Hasinger, G. 2003, proceedings of the Conference: The Emergence of Cosmic Structure, Maryland, Stephen S. Holt and Chris Reynolds (eds), astro-ph/0302574
22. Schmidt, M. et al. 1998, A&A, 329, 495
23. Lehmann, I., et al. 2001, A&A, 371, 833
24. Cowie L., Barger A., Bautz, M.W., Brandt, W.N., & Garnire, G.P. 2003, ApJ, 584, L57
25. Fiore, F., et al. 2000, NewA, 5, 143
26. Comastri, A. et al. 2002, ApJ, 571, 771
27. Baldi, A., Molendi, S., Comastri, A., Fiore, F., Matt, G., & Vignali, C. 2002, ApJ, 564, 190
28. Kim, D-W. et al. 2003, ApJS in press, astro-ph/0308492
29. Harrison, F.A., Eckart, M.E., Mao, P.H., Helfand, D.J., Stern, D. 2003, ApJ, in press, astro-ph/0306610
30. Elvis, M., Fiore, F., Wilkes, B.J., McDowell, J.C. & Bechtold, J., 1994, ApJ, 422, 60.
31. Fiore, F., Elvis, M., Giommi, P. & Padovani, P., 1998, ApJ, 492, 79.
32. Brusa, M., Comastri, A., Mignoli, M. et al. 2003, A&A in press, astro-ph/0307368
33. Page M.J, McHardy I.M., Gunn K.F. et al. 2003, AN, 324, 101
34. Maiolino, R., Marconi, A., Oliva, E. 2001, A&A 365, 37
35. Frontera F. et al., 1997, A&AS, 112, 357
36. Matt, G., Fabian, A. C., Guainazzi, M., Iwasa, K., Bassani, L., Malaguti, G. 2000, MNRAS, 318, 173
37. Risaliti, G. 2002, A&A, 386, 379
38. Vignati, P. et al. 1999, A&A, 349, L57
39. Franceschini, A., Hasinger, G., Miyaji, T., & Malguori, D. 1999, MNRAS, 310, L5
40. Maiolino, R. et al. 1998, A&A, 338, 781
41. Mainieri, V. et al. 2002, A&A, 393, 425
42. Grossan, B.A. 1992, Ph.D. thesis, MIT
43. Schmidt, M. 1968, ApJ, 151, 393
44. Hartwick, F.D.A., & Schade, D. 1990, ARA&A, 28, 437
45. Fabian, A.C. 2003, Carnegie Observatories Astrophysics Series, Vol. I, ed. L. Ho., Cambridge University Press, astro-ph/0304122
46. Gebhardt, K., Kormendy, J., & Ho, L. et al. 2000, ApJ, 543, L5
47. Ferrarese, L. & Merritt, D. 2000, ApJ, 539, L9